Published January 19, 2015

VEGF-A modulates expression of inhibitory checkpoints on CD8+ T cells in tumors

Thibault Voron,[1,4*] Orianne Colussi,[1,5*] Elie Marcheteau,[1*] Simon Pernot,[1,5] Mevyn Nizard,[1] Anne-Laure Pointet,[1,5] Sabrina Latreche,[1] Sonia Bergaya,[1] Nadine Benhamouda,[2] Corinne Tanchot,[1] Christian Stockmann,[1] Pierre Combe,[3] Anne Berger,[4] Franck Zinzindohoue,[4] Hideo Yagita,[6] Eric Tartour,[1,2] Julien Taieb,[1,5*] and Magali Terme[1*]

[1]INSERM U970, Paris Cardiovascular Research Center, Université Paris-Descartes, Sorbonne Paris Cité, 75015 Paris, France
[2]Service d'immunologie biologique, [3]Service d'oncologie médicale, [4]Service de chirurgie digestive, [5]Service d'hépatogastroentérologie et d'oncologie digestive, Hôpital Européen Georges Pompidou, 75015 Paris, France
[6]Department of Immunology, Juntendo University School of Medicine, Tokyo 113-8421, Japan

Immune escape is a prerequisite for tumor development. To avoid the immune system, tumors develop different mechanisms, including T cell exhaustion, which is characterized by expression of immune inhibitory receptors, such as PD-1, CTLA-4, Tim-3, and a progressive loss of function. The recent development of therapies targeting PD-1 and CTLA-4 have raised great interest since they induced long-lasting objective responses in patients suffering from advanced metastatic tumors. However, the regulation of PD-1 expression, and thereby of exhaustion, is unclear. VEGF-A, a proangiogenic molecule produced by the tumors, plays a key role in the development of an immunosuppressive microenvironment. We report in the present work that VEGF-A produced in the tumor microenvironment enhances expression of PD-1 and other inhibitory checkpoints involved in CD8+ T cell exhaustion, which could be reverted by anti-angiogenic agents targeting VEGF-A–VEGFR. In view of these results, association of anti-angiogenic molecules with immunomodulators of inhibitory checkpoints may be of particular interest in VEGF-A-producing tumors.

CORRESPONDENCE
Julien Taieb:
julien.taieb@egp.aphp.fr

Abbreviations used: BTLA, B- and T-lymphocyte attenuator; CsA, cyclosporin A; CTLA-4, cytotoxic T-lymphocyte-associated protein 4; Flt3, Fms-like tyrosine kinase 3; LAG-3, lymphocyte activation gene-3; MDSC, myeloid-derived suppressor cells; NFAT, nuclear factor of activated T-cells; PD-1, Program Death-1; Pi3K, phosphatidylinositide 3-kinase; PLCγ, phospholipase C γ; TKI, tyrosine kinase inhibitor; T reg cell, regulatory T cells; VEGF, vascular endothelial growth factor; VEGFR, VEGF receptor.

One of the major processes involved in tumor appearance and growth is the capacity of tumor cells to develop escape mechanisms to the immune system (Schreiber et al., 2011). Thus, induction of cells with immunosuppressive properties, such as regulatory T (T reg) cells or myeloid-derived suppressor cells (MDSCs), and promotion of T cell exhaustion are key mechanisms of immune evasion. T cell exhaustion is phenotypically characterized by the expression of inhibitory molecules called inhibitory checkpoints, such as Program Cell Death-1 (PD-1), and functionally by a gradual dysfunction state where effector functions of T cells are blocked. Studies have shown that PD-1–PD-L1 pathway blockade could improve antitumor immune responses in mouse models (Sakuishi et al., 2010). Administration of anti–PD-1 antibody to metastatic melanoma patients leads to durable objective responses in 17–28% of patients. These responses are associated with an increase in CD8+ T cell infiltration (Topalian et al., 2012; Hamid et al., 2013). Thus, blocking the PD-1 pathway could help to overcome T cell exhaustion and restore efficient antitumor responses. In tumors or during chronic viral infections, PD-1 expression is maintained (Wherry et al., 2007). The mechanisms involved in PD-1 expression and exhaustion of tumor-infiltrating T cells are poorly understood, even though a link to antigen persistence has been suggested (Wherry, 2011). Factors produced in the tumor microenvironment could be involved in the induction of PD-1 expression, and thereby of exhaustion in the tumors, for the following reasons: only tumor-infiltrating CD8+ T cells and noncirculating CD8+ T cells bear an exhausted phenotype and express PD-1 (Baitsch et al., 2011);

*T. Voron, O. Colussi, E. Marcheteau, J. Taieb, and M. Terme contributed equally to this paper.

The Rockefeller University Press $30.00
J. Exp. Med. 2015 Vol. 212 No. 2 139–148
www.jem.org/cgi/doi/10.1084/jem.20140559

Published January 19, 2015

and vaccination protocols have been shown to stimulate antigen-specific CD8+ T cells in tumor patients, but these CD8+ T cells remain hyporesponsive at the tumor site (Appay et al., 2006). Among immunosuppressive factors produced by tumor cells, VEGF-A exhibits proangiogenic properties but also has a key role in the induction of an immunosuppressive microenvironment (inhibition of dendritic cell maturation, accumulation of MDSC, and induction of T reg cells; Gabrilovich et al., 1996; Huang et al., 2007). We have recently shown that VEGF-A could also directly induce T reg cell proliferation in a VEGFR2-dependent manner in tumor-bearing mice and metastatic colorectal cancer patients (Terme et al., 2013). Targeting the VEGF-A–VEGFR axis with antiangiogenic molecules could decrease T reg cell and MDSC proportions in tumor-bearing mice and cancer patients (Finke et al., 2008; Ko et al., 2009; Cao et al., 2011; Terme et al., 2013). Sunitinib, a multitarget tyrosine kinase inhibitor (TKI) that blocks vascular endothelial growth factor receptors 1, 2, and 3 (VEGFR1, R2, and R3), platelet-derived growth factor receptors α and β, stem cell factor receptor, and Flt3, has been shown to decrease PD-1 expression at the mRNA level in tumor-infiltrating T cells (Ozao-Choy et al., 2009). However, it is unclear whether the effect of this multitarget molecule results directly from VEGF-A–VEGFR axis inhibition or through another signaling mechanism. In vitro studies have shown that VEGF-A could decrease T cell functions (Gavalas et al., 2012; Ziogas et al., 2012) without addressing the direct role of VEGF-A on the regulation of PD-1 expression and thereby on T cell exhaustion in tumors. Thus, we studied the impact of VEGF-A–VEGFR blockade on PD-1 and other inhibitory receptor expression on CD8+ T cells and the direct role of tumor-derived VEGF-A on tumor-induced T cell exhaustion.

RESULTS AND DISCUSSION

Targeting VEGF-A–VEGFR pathway is sufficient to decrease PD-1 expression on intratumoral CD8+ T cells

We first analyzed the impact of VEGF-A–VEGFR blockade on PD-1 expression on tumor-infiltrating CD8+ T cells in a mouse model of colorectal cancer (CT26). CT26 tumor cells produce high levels of VEGF-A in vitro (Terme et al., 2013). In vivo, the VEGF-A concentration was ∼10 times higher in the tumor microenvironment, reaching 366.9 ± 53.8 pg/ml as compared with plasma level (31.4 ± 4.38 pg/ml). In the same way, PD-1 expression was low on splenic CD8+ T cells from naive (3.12 ± 2.60%) and tumor-bearing mice (3.27 ± 2.43%), but strongly increased on intratumoral CD8+ T cells (54.85 ± 16.16 pg/ml; $P < 0.0001$). CT26 tumor-bearing mice were treated with anti–VEGF-A antibody or different TKI targeting (sunitinib) or not (masitinib) VEGFR. DMSO or mouse serum were given to mice as control for TKI and anti–VEGF-A antibody, respectively, without modulating PD-1 expression compared with nontreated tumor-bearing mice (unpublished data). Treatments targeting the VEGFA–VEGFR axis resulted in a significant reduction of PD-1 expression on intratumoral CD8+ T cells, whereas masitinib (Fig. 1, a–c, right), a TKI that targets c-Kit, PDGFR, and Fak kinases but not VEGFR (Dubreuil et al., 2009), had no effect. These treatments induced significant antitumor effects (Fig. 1, a and b, left). Thus, blocking VEGF-A–VEGFR axis decreases PD-1 expression on intratumoral CD8+ T cells and restores IFN-γ production in intratumoral CD8+ T cells (28.35 ± 5.7% in control group and 62.11 ± 5.3% in anti-VEGFA–treated mice after PMA/ionomycin restimulation; $P = 0.0015$). Interestingly, the antitumor effect of anti-VEGFA is at least in part due to CD8+ T cells because depletion of CD8+ T cells reduced antitumor effect during anti-VEGFA treatment (Fig. 1 d). We next looked for evidence of VEGF-A involvement in PD-1 expression and found that the intratumoral VEGF-A level was significantly correlated with PD-1 expression on tumor-infiltrating CD8+ T cells (Fig. 1 e; $r = 0.502$; $P = 0.0398$). We also took advantage of a fibrosarcoma cell line nullizygous for VEGF-A expression (Stockmann et al., 2008). Importantly, in VEGF-null tumors (MEF KO), the percentage of PD-1 expression on intratumoral CD8+ T cells was greatly decreased compared with MEF wild-type counterparts (Fig. 1 f).

VEGF-A enhances PD-1 expression on VEGFR-expressing CD8+ T cells in vitro

To understand whether VEGF-A can act directly on CD8+ T cells, we first analyzed the expression of the two VEGF-A receptors, VEGF-R1 and -R2, on CD8+ T cells in vivo. We observed that these two receptors are expressed only at very low levels in spleens of tumor-free and tumor-bearing mice, but are strongly increased on tumor-infiltrating CD8+ T cells (Fig. 2 a). These VEGFR+ CD8+ T cells also expressed PD-1 (unpublished data). Because tumor-infiltrating T cells bear an activated phenotype unlike splenic CD8+ T cells, these results suggested that VEGFR expression could be associated with T cell activation (Whiteside and Parmiani, 1994). To recapitulate this phenomenon in vitro, we analyzed expression of these receptors after stimulation of purified CD8+ T cells with different doses of anti-CD3 by flow cytometry and confocal microscopy. Expression of VEGF-R1 and -R2 was induced by stimulation with 3 µg/ml of anti-CD3 and became significant at 10 µg/ml after 48 h of culture (Fig. 2, b–d). Because CD8+ T cells can express VEGF receptors after activation, we then analyzed the impact of VEGF-A on these T cells. Anti-CD3 stimulation induced expression of PD-1, but addition of VEGF-A enhanced PD-1 expression on these cells in a dose-dependent manner (Fig. 2, e–f). Furthermore, this effect was blocked when anti–VEGF-A antibody was added to the culture (unpublished data). Thus, VEGF-A directly increases PD-1 expression on activated CD8+ T cells.

VEGF-A directly enhances expression of inhibitory receptors involved in T cell exhaustion

PD-1 is the first inhibitory receptor associated with T cell exhaustion. However, other receptors are expressed on exhausted T cells, such as Tim-3, CTLA-4, and Lag-3 (Sakuishi et al., 2010; Woo et al., 2012; Duraiswamy et al., 2013). Density and co-expression of these different molecules have been associated with the magnitude of T cell exhaustion. The more

Published January 19, 2015

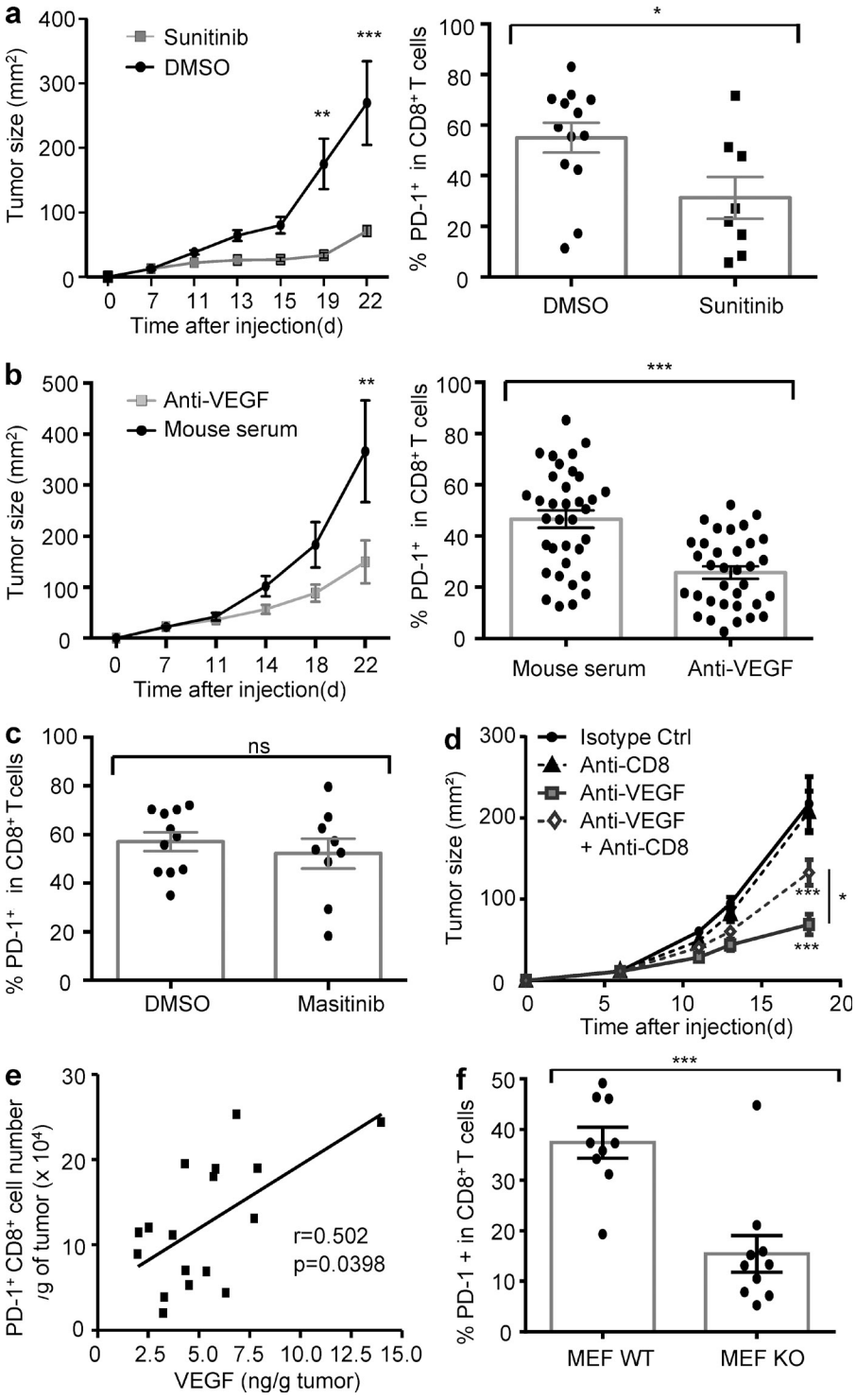

Figure 1. VEGF-A–VEGFR inhibition decreases PD-1 expression on intratumoral CD8⁺ T cells. CT26 tumor-bearing mice were treated with sunitinib or DMSO (as a control; a), or anti-VEGF-A antibody or mouse serum (as a control; b), or masitinib or DMSO (as a control; c). Treatments were started when tumors reached 9–10 mm². Tumor growth (left) was shown. Mice were sacrificed at day 22 after 2 wk of treatment, and PD-1 expression on tumor-infiltrating CD8⁺ T cells was analyzed (right). Each dot represents an individual mouse, and histograms represent mean ± SEM of 2–4 pooled experiments with at least 4 mice/group. *, P = 0.0439; ***, P < 0.001. (d) Depletion of CD8⁺ T cells decreases anti-VEGFA–induced antitumor effects. (e) Correlation of VEGF-A concentration/gram of tumor tissue and number of PD-1-expressing CD8⁺ T cells/gram of tumor tissue (determined by flow cytometry). Each dot represents an individual tumor sample. (f) PD-1 expression on tumor-infiltrating CD8⁺ T cells was analyzed on wild-type MEF-tumor bearing mice (MEF WT) and VEGF-A–deleted MEF cells (MEF KO) after 14 d of tumor growth. Each dot represents an individual mouse. Histograms represent mean ± SEM of 2 pooled experiments with 4–5 mice/group. For tumor growths, one representative experiment out of 3 is shown with 5 mice/group. **, P < 0.01; ***, P < 0.001.

the T cells express these receptors the more they are dysfunctional (Blackburn et al., 2009). We observed that VEGF-A not only enhances PD-1 expression but also increases the percentages of Tim-3– and CTLA-4–expressing CD8⁺ T cells in a dose-dependent manner (Fig. 3, a–c). The levels of the expression for each molecule (PD-1, Tim-3, CTLA-4, and Lag-3) were also increased in a dose-dependent manner (Fig. 3 d). We then analyzed the simultaneous co-expression of these receptors. Strikingly, compared with the basal expression of 0–1 inhibitory receptor expressed on CD8⁺ T cells in the absence of exogenous VEGF-A, increasing VEGF-A concentrations induced the simultaneous expression of 3–4 inhibitory receptors on more than 2/3 of T cells (Fig. 3 e). To determine whether VEGF-R1 or VEGF-R2 are involved in

Published January 19, 2015

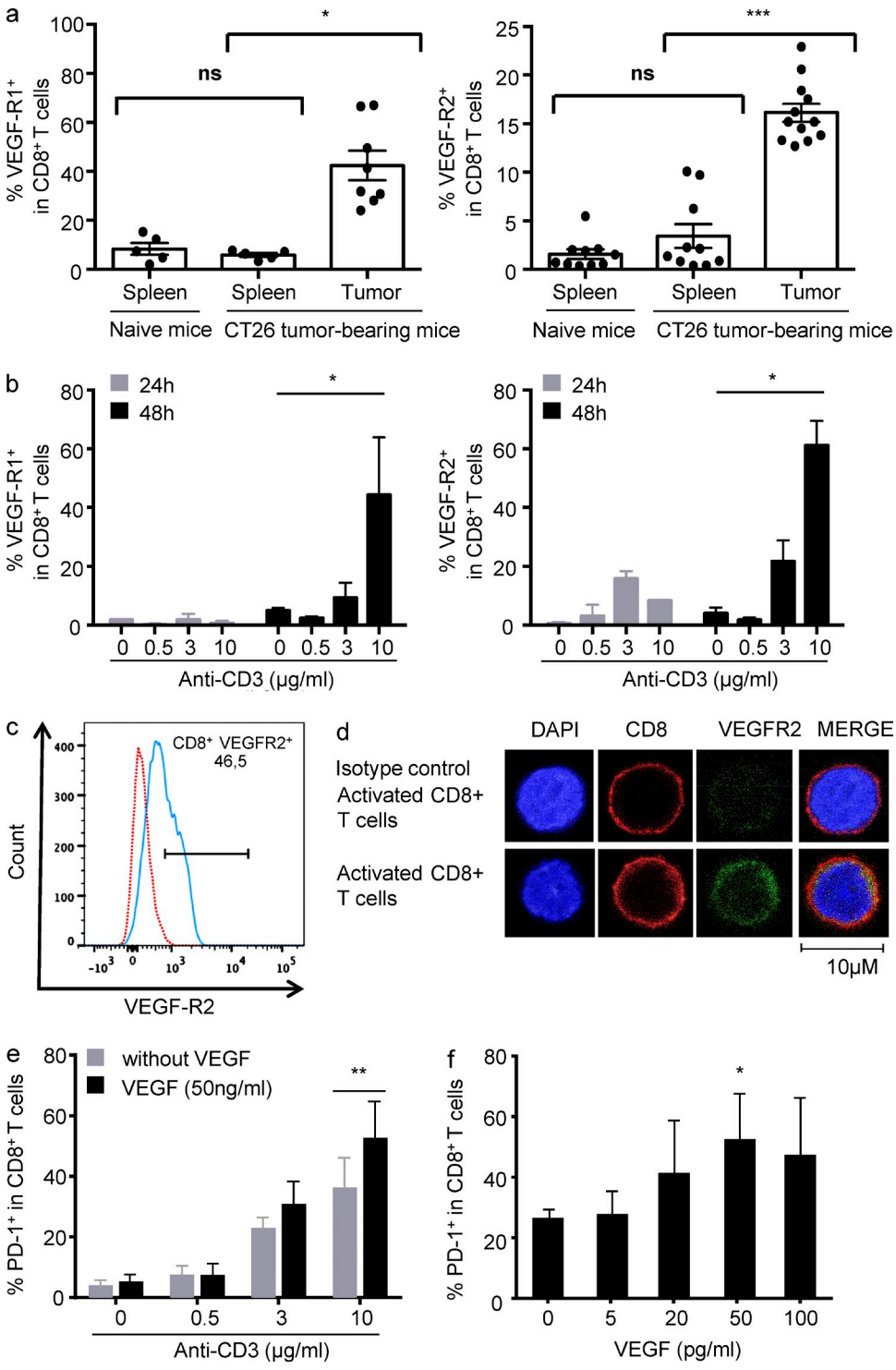

Figure 2. VEGF-A enhances PD-1 expression on CD8⁺ T cells in vitro. (a) VEGF-R1 (left) and -R2 (right) expression is shown on CD8⁺ T cells from tumors and spleen of tumor-free (naive) and CT26 tumor-bearing mice. Each dot represents an individual mouse, histograms represent mean ± SEM of 2 pooled experiments with 3–5 mice/group. (b) VEGF-R1 (left) and -R2 (right) expression on purified CD8⁺ T cells after 24 and 48 h of culture with various doses of plate-bound anti-CD3 antibody. (c and d) Same experimental setting as in b, but showing a representative staining of VEGF-R2 by flow cytometry (c) and confocal microscopy (d). Isotype control of anti-VEGFR2 antibody is shown (blue line for c and top for d). (e) PD-1 expression on purified CD8⁺ T cells after 48 h of culture with plate-bound anti-CD3 with or without VEGF-A (50 ng/ml). (f) Same experiment as in e but with 10 µg/ml of plate-bound anti-CD3 and various doses of VEGF-A. *, $P < 0.05$; **, $P < 0.01$; ***, $P < 0.001$.

Published January 19, 2015

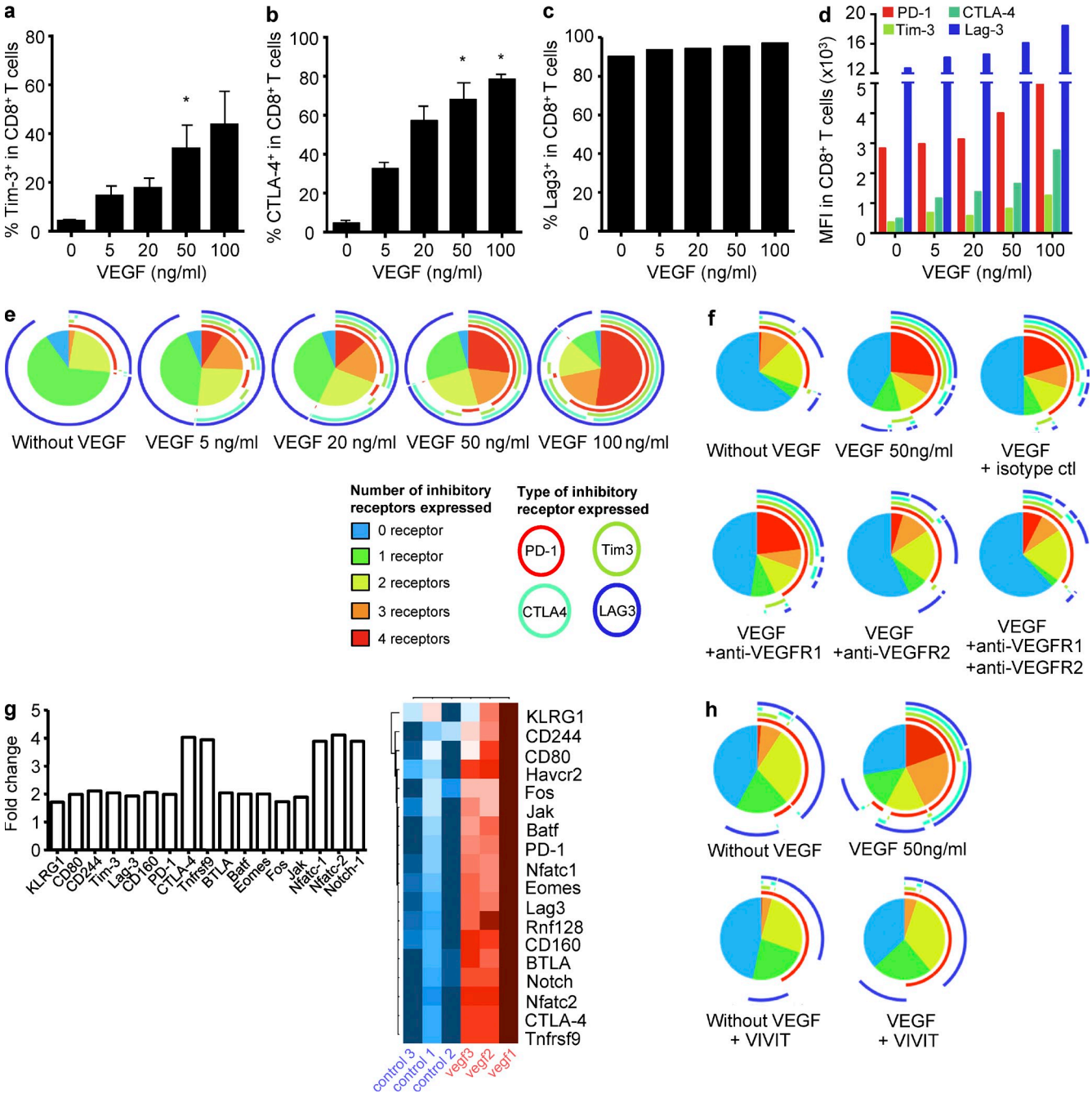

Figure 3. VEGF-A enhances co-expression of inhibitory receptors involved in CD8⁺ T cell exhaustion in a VEGF-R2 and NFAT-dependent manner. Percentages of Tim-3 (a), CTLA-4 (b), and Lag-3 (c) expression on purified CD8⁺ T cells after 48 h of culture with plate-bound anti-CD3 (10 µg/ml) and various doses of VEGF-A. Histograms represent means ± SEM of 3 pooled experiments. (d) Same experimental settings as in (a) but mean fluorescence intensity (MFI) is shown. (e) The simultaneous expression of inhibitory receptors (PD-1, Tim-3, CTLA-4, and Lag-3) was examined on stimulated CD8⁺ T cells. (f) Same experimental setting as in (e) but in the presence of anti-VEGF-R1 or -R2 antibodies. (g) Transcriptional analyses of gene products linked to T cell exhaustion and VEGF-R2 signaling in CD8⁺ T cells stimulated or not with VEGF-A using a microfluidic card designed for qRT-PCR (TaqMan Low Density Mouse Immune Array from Applied Biosystems). Graph represents log fold changes (relative to nontreated controls, calculated with the ΔΔCT method (normalization with RNA18s as endogenous control) of transcripts. (h) Same experimental setting as in (e) in the presence of 11R-VIVIT. For simultaneous expression of inhibitory receptors, one representative experiment out of three is shown. *, $P < 0.05$.

VEGF-A–mediated T cell exhaustion, we added neutralizing antibodies to the CD8⁺ T cell culture in the presence of VEGF-A. Anti–VEGF-R2, but not anti–VEGF-R1 antibody, was able to block the VEGF-A–induced up-regulation of these inhibitory receptors (Fig. 3 f), demonstrating the involvement of VEGF-R2 in this phenomenon. To extend this

Published January 19, 2015

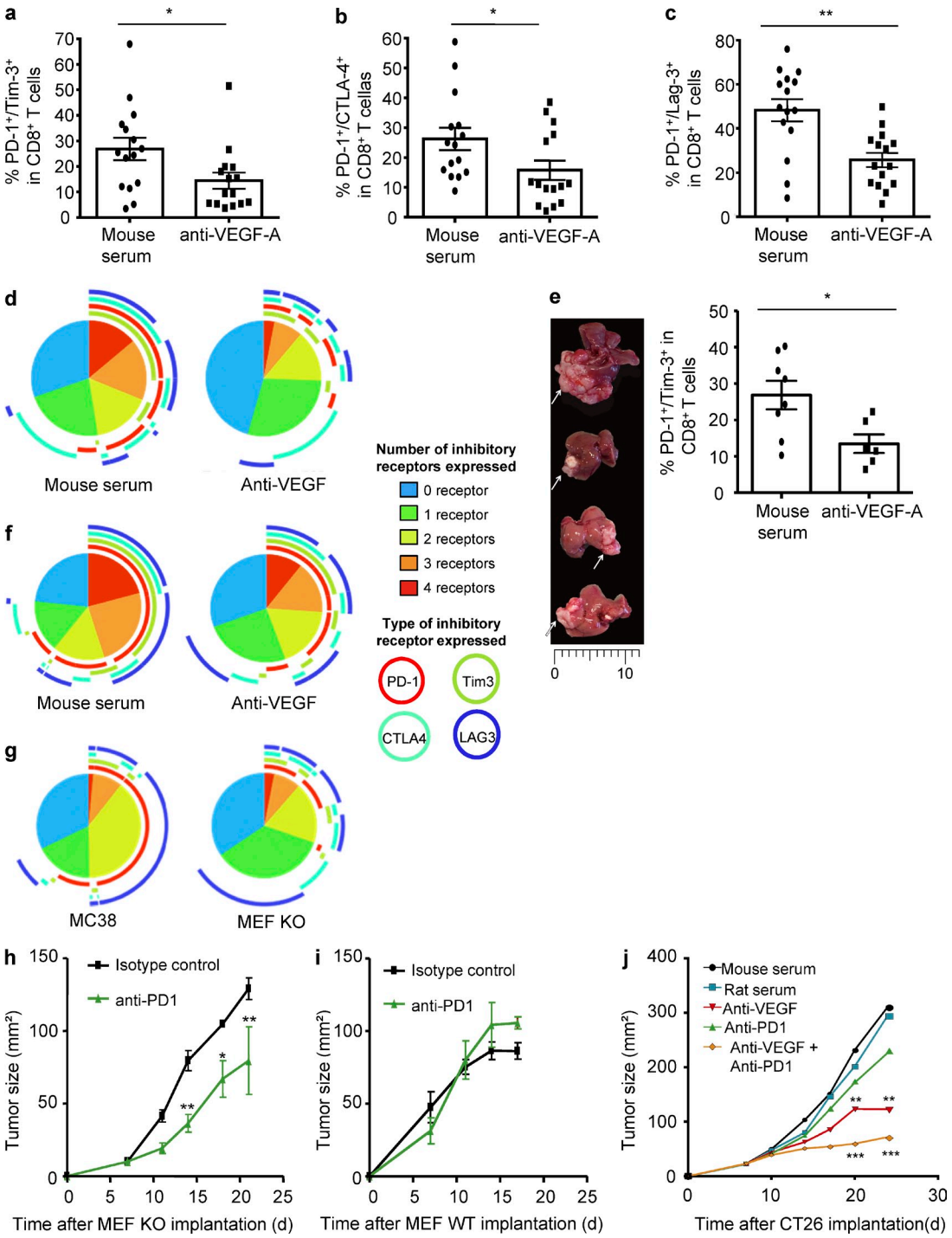

Figure 4. VEGF-A neutralization decreases expression of inhibitory receptors involved in exhaustion on CD8⁺ T cells in heterotopic and orthotopic mouse tumor models. Mice bearing subcutaneous CT26 tumors were treated with anti-VEGF-A antibody or mouse serum (as a control). Co-expressions of PD-1/Tim-3 (a), PD-1/CTLA-4 (b), or PD-1/Lag-3 (c) on intratumoral CD8⁺ T cells have been analyzed. 3 pooled experiments are shown with 5 mice/group. *, $P < 0.05$; **, $P < 0.01$. (d) Co-expression of PD-1, Tim-3, CTLA-4, and Lag-3 has been determined on intratumoral CD8⁺ T cells after 14 d of anti-VEGFA treatment (day 22). (e) Anti-VEGF-A was given to mice bearing CT26 hepatic metastases. Representative pictures of hepatic metastases (left panel) and the percentages of intratumoral CD8⁺ T cells expressing PD-1/Tim-3 (right panel) were shown. Two pooled experiments are shown with 3–4 mice/group. *, $P < 0.05$ (f). Same experimental setting as in d, but on CT26 hepatic metastases. (g) Co-expression of inhibitory receptors on CD8⁺ T from MC38 and MEF KO tumors. (h–i) VEGF-KO MEF (h) and wild-type MEF tumor-bearing mice (i) were treated with anti–PD-1 alone twice a week starting at day 7. (j) CT26 tumor-bearing mice were treated with anti-VEGFA or anti–PD-1 alone or both. Tumor growth was monitored twice a week. One representative experiment out of three is shown, with five mice per group. *, $P < 0.05$; **, $P < 0.01$; ***, $P < 0.001$.

Published January 19, 2015

observation, we analyzed the differential expression of genes coding for inhibitory receptors involved in CD8$^+$ T cell exhaustion. Quantitative RT-PCR analysis showed that other inhibitory receptors, such as CD244/2B4, CD160, and BTLA, were also enhanced by VEGF-A stimulation (Fig. 3 g). These results showed that VEGF-A enhances expression of many different inhibitory receptors involved in CD8$^+$ T cell exhaustion. Furthermore, an increased expression of NFAT was observed after VEGF-A stimulation (Fig. 3 g). NFAT is known to be involved in VEGF-R2 signaling (Liu et al., 2003; Schweighofer et al., 2009), as well as in the control of PD-1 and CTLA-4 expression (Gibson et al., 2007; Oestreich et al., 2008). To determine if VEGF-A–induced T cell exhaustion is dependent on NFAT activation, we used a specific NFAT inhibitor (11R-VIVIT; Le Roy et al., 2012). Interestingly, NFAT inhibition blocked the VEGF-A–induced simultaneous expression of the 4 inhibitory receptors (Fig. 3 h). Among the different signaling pathways activated by VEGFR2 (PI3K–Akt, PLCγ, and Erk), the PLCγ–calcineurin pathway is known to activate NFAT (Schweighofer et al., 2009). Upon VEGF-A treatment, increased PLCγ phosphorylation was observed in CD8$^+$ T cells by Western blot (unpublished data). Furthermore, inhibition of PLCγ and calcineurin by the chemical inhibitor U73122 and cyclosporine A (CsA), respectively, resulted in an inhibition of VEGF-A–induced inhibitory receptor expression on CD8$^+$ T cells (unpublished data). Together, these results show that VEGF-A enhances the expression of inhibitory receptors involved in T cell exhaustion via activation of the VEGFR2–PLCγ–calcineurin–NFAT pathway.

Targeting VEGF-A in tumor models reverts expression of inhibitory molecules associated with T cell exhaustion

To document if VEGF-A neutralization could revert expression of PD-1 and other inhibitory receptors in vivo, we tested anti–VEGF-A treatment on CT26-bearing mice. CT26 cells were implanted subcutaneously but also directly to the liver by subcapsular injection of tumor cells in the left lobe of the liver resulting in the development of liver metastases within 7–10 d, which is more relevant than our subcutaneous tumor model. Consistent with our in vitro results, VEGF-A inhibition decreased the proportion of tumor-infiltrating CD8$^+$ T cells expressing PD-1/Tim-3, PD-1/CTLA-4, and PD-1/Lag-3 (Fig. 4, a and c). Analysis of simultaneous expression of these receptors on CD8$^+$ T cells revealed that anti–VEGF-A treatment decreased the proportion of tumor-infiltrating CD8$^+$ T cells expressing 3–4 receptors when treatment was started when tumors reached ∼10 mm^2 (Fig. 4 d). It is of note that anti–VEGF-A treatment has no effect on the expression of 3–4 inhibitory receptors on tumor-infiltrating CD8$^+$ T cells when very large tumors were treated (>90 mm^2 at the beginning of the treatment). Mice bearing hepatic metastases (Fig. 4 e, left) were treated with anti–VEGF-A from day 10–20. Analysis of inhibitory receptors revealed a decrease of CD8$^+$ T cells bearing 3–4 inhibitory receptors and mainly of PD-1/Tim-3 expression confirming our results in this more relevant tumor site (Fig. 4, e and f). Interestingly, in two tumor models where intratumoral VEGF-A level is low, VEGF-null tumors (MEF-KO) and the MC38 colorectal tumor model (133.3 ± 15.35 pg/ml), the proportion of tumor-infiltrating CD8$^+$ T cells expressing 3–4 inhibitory receptors was limited (<25%; Fig. 4 g). Together, these results showed that targeting VEGF-A can decrease the VEGF-induced expression of inhibitory receptors mediating CD8$^+$ T cell exhaustion, not only in subcutaneously established tumors, but also in hepatic metastases from colorectal cancer.

Combination of anti–PD-1 antibodies with VEGF-A blockade induced a strong and synergic antitumor effect in tumors producing high levels of VEGF-A

Immunotherapeutic strategies using anti–PD-1 antibodies have been recently developed and resulted in strong antitumor responses in advanced solid tumors (Topalian et al., 2012). However, not all patients experienced an objective response. Because anti–VEGF-A treatment decreases PD-1 expression on intratumoral CD8$^+$ T cells but does not fully restore the steady-state level of PD-1 expression, we hypothesized that VEGF-A blockade could help to sensitize T cells to anti–PD-1 antibody treatment in some tumors. We administered anti–PD-1 antibody to VEGF-deleted-MEF tumor cells (Fig. 4 h) or wild-type MEF tumor cells (Fig. 4 i). Interestingly, anti–PD-1 antibody induced a significant antitumor effect only in VEGF-KO MEF tumor-bearing mice (Fig. 4 h) and not in WT MEF tumor-bearing mice (Fig. 4 i), suggesting that VEGF produced by tumor cells limits anti–PD-1–induced antitumor effects. We next tried to combine anti-VEGFA antibody with anti–PD-1 antibody in our CT26 mouse model of colorectal cancer expressing high levels of VEGF-A (Fig. 4 j). Anti–VEGF-A treatment reduced tumor growth ($P < 0.0001$; Fig. 1 b), and anti–PD-1 antibody alone had no significant effect, but the anti–VEGF-A and anti–PD-1 combination induced a strong antitumor effect (71.91 ± 64.66 mm^2) as compared with anti–VEGF-A alone (123 ± 56.21 mm^2; $P = 0.05$) or anti-PD-1 alone (227 ± 28.9 mm^2; $P = 0.05$). This result suggests that high VEGF-A levels may be involved in resistance to anti–PD-1 treatments and that anti-angiogenic therapies targeting VEGF-A–VEGFR in these tumors expressing high levels of VEGF-A could synergize with anti–PD-1 treatment strategies and enhance anti–PD-1–dependent antitumor effects.

Our work shows, to our knowledge for the first time, that VEGF-A produced by the tumor enhances expression of inhibitory immune checkpoints mediating T cell exhaustion on intratumoral CD8$^+$ T cells. In vivo analysis of VEGFR expression in mouse tumor models revealed that only tumor-infiltrating activated CD8$^+$ T cells, and not circulating CD8$^+$ T cells, can express VEGFR, which seems to be linked to TCR engagement. In vitro, addition of VEGF-A after TCR engagement on CD8$^+$ T cells increases expression of inhibitory checkpoints (PD-1, Tim-3, CTLA-4, and Lag-3) in a VEGFR-2/PLCγ/calcineurin/NFAT-dependent manner. In CT26 heterotopic and liver metastases tumor models where intratumoral VEGF-A level is high, anti–VEGF-A treatment

Published January 19, 2015

could down-regulate the expression of these inhibitory receptors. Combining antiangiogenic agents targeting the VEGF-A–VEGF-R2 axis could synergize with immunotherapeutic approaches, as shown here, by combining anti–VEGF-A with anti-PD-1 in VEGF-expressing tumors, which are resistant to anti-PD-1 treatment. As in mouse tumor models, tumor-infiltrating $CD8^+$ T cells, but not circulating $CD8^+$ T cells, derived from colorectal cancer patients express VEGFR2 (48.4 ± 14.25%). Further investigations are needed to determine if VEGF-A could modulate inhibitory receptor expression on human $CD8^+$ T cells.

MATERIALS AND METHODS

Animals

6–8-wk-old female BALB/c or C57BL/6 mice were purchased from Charles River Laboratories and kept in specific pathogen–free conditions at the Institut National de la Santé et de la Recherche Médicale U970 animal facility. Experiments respected institutional guidelines and were approved by the Paris-Descartes University ethics committee (CEEA34.MT.072.12).

Animal models and treatments

Heterotopic tumor models. Two-colon carcinoma models were used: CT26 and MC38. CT26, an *N*-nitroso-*N*-methylurethane-induced undifferentiated colon carcinoma cell line, was obtained from American Type Culture Collection and MC38 was provided by N. Chaput (Insitut Gustave-Roussy, France). VEGF KO and wild-type MEF cells were provided by C. Stockmann (INSERM, Paris, France). The VEGF-A–deficient MEFs are isogenic with the wild-type MEFs (Stockmann et al., 2008). CT26 cells (2×10^5) or VEGF-KO MEF and wild-type MEF cells (10^6) or MC38 (5×10^5) were injected subcutaneously at day 0 in the right flank of BALB/c mice (CT26) or C57BL/6 mice. Tumor growth was monitored twice a week using a caliper.

Model of colorectal liver metastases. At day 0, the BALB/c mice were anesthetized with i.p. injection of 100 µl of ketamine/xylazine and operated on through a midline laparotomy. After liver exposure, a single liver tumor was induced by direct injection of 1.5×10^4 CT26 cells under the liver capsule of the left lobe. The midline incision was closed with interrupted suture. At day 10, all mice were randomized between the control and the treated groups before treatment. At day 24, mice were sacrificed.

Treatments. Treatments were started when the tumors reached 9–10 mm^2. Sunitinib (Sutent) and masitinib (4-[4-methylpiperazin-1-ylmethyl]-*N*-[4-methyl-3-[4-pyridin-3ylthiazol-2-ylamino] phenyllbenzamide-mesylate methane sulfonic acid salt) were given by oral gavage at 40 mg/kg daily and 30 mg/kg bid, respectively. Sunitinib and masitinib were dissolved in DMSO and diluted in PBS before administration. Control mice received DMSO diluted in PBS. In this study, masitinib was used as a negative control to probe the VEGFR inhibition of sunitinib. Masitinib is a highly selective TKI that targets a limited number of key kinases involved in various cancers and inflammatory diseases, including c-Kit, PDGFR and Fak, but not VEGFR (Dubreuil et al., 2009). Masitinib is currently the most selective TKI in clinical development or already approved to date. An anti–mouse-VEGF-A antibody (B20-4.1.1) was administered i.p. at 5 mg/kg twice a week.

In some experiments, a neutralizing anti–mouse PD-1 antibody (RPM1-14; Yamazaki et al., 2005) was administered i.p. at 0.25 mg twice a week. Sunitinib was provided by Pfizer, anti–mouse-VEGF-A antibody was provided by Genentech, and masitinib was provided by AB Science SA. After treatments, tumors were dissociated using Gentle Macs dissociator (Miltenyi Biotec). For $CD8^+$ T cell depletion studies, anti-CD8 antibody (clone 2.43; BioXcell) or isotype control antibody (rat IgG2a) was administered at 100 µg i.p. to CT26-tumor bearing mice the day before starting anti-VEGFA treatment. CD8 depletion was checked by flow cytometry.

Flow cytometry

Cell surface-staining was performed on tumor-infiltrating cells using anti-CD8 (53–6.7; eBioscience), anti–PD-1 (J43; eBioscience), anti–CTLA-4 (UC10-4B9; BioLegend), anti–Lag-3 (C9B7W; BioLegend), anti–Tim-3 (RMT3-23; BioLegend), anti–mouse VEGF-R2 (89B3A5; BioLegend), and anti–mouse VEGF-R1 (141522; R&D Systems). Isotype controls were used as a negative control. Dead cells were excluded using live/dead fixable aqua dead cell kit (Invitrogen, UK). Stained cells were analyzed with LSRII cytofluorometer using FACS Diva Software (BD), and FlowJo Software (Tree Star). The co-expression of inhibitory molecules was analyzed using SPICE v5.3 software.

Confocal microscopy

Anti-CD3–stimulated $CD8^+$ T cells were stained for confocal microscopy. In brief, cells were fixed in 2% paraformaldehyde on superfrost plus slides. Cells were washed 3 times in PBS-Triton X-100 0.1%, and then blocked with PBS containing BSA and glycin for 30 min before incubation with primary antibodies: anti-VEGFR2 (55B11; Cell Signaling Technology) or anti-CD8 (clone 53–6.7; eBioscience), or isotype control antibodies (rabbit IgG isotype control (Cell Signaling Technology) and rat IgG2a isotype control (eBioscience). Cells were then washed with PBS Triton 0.1% and incubated with secondary antibodies: goat anti–rabbit Alexa Fluor 647 and goat anti–rat Alexa Fluor 488 (Life Technologies). After washing, cells were incubated with DAPI and mounted over Fluoromount G (Interchim). Confocal microscopy was performed using the SP8 Leica microscope using LAS AF software (Leica) and ImageJ software.

VEGF dosage

Tumors were mechanically dissociated with lysis buffer (T-PER Tissue Protein Extraction Reagent; Thermo Fisher Scientific) containing a protease inhibitor (Halt Protease Inhibitor Cocktail, EDTA-Free; Thermo Fisher Scientific). For each tumor model, the same quantity of tumors has been dissociated in the lysis buffer (100 mg of tumors in 2 ml of lysis buffer). Supernatant was obtained after centrifugation. VEGF-A concentration was evaluated by ELISA (mouse VEGF DuoSet; R&D Systems).

Isolation and culture of lymphocytes

$CD8^+$ T lymphocytes were purified from splenocytes using a $CD8^+$ isolation kit (Miltenyi Biotec). Purified $CD8^+$ T lymphocytes were cultured in the presence of plate-bound anti-CD3 (10 µg/ml) with or without recombinant murine VEGF-A (50 ng/ml; Miltenyi Biotec). After 48 h of culture, cells were harvested and analyzed by cytometry or used to extract mRNA. In some experiments, anti–VEGF-R1 (20 µg/ml; R&D Systems) or anti–VEGF-R2 (10 µg/ml; clone 91202; R&D Systems) antibodies or isotype control were added to the culture medium. In some experiments, 11R-VIVIT (Merck Millipore) was added 1 h at 5 µM before the addition of VEGF-A and during the stimulation with VEGF-A.

RNA sample preparation and quantitative RT-PCR analyses

Total RNA from VEGF-A-treated or nontreated $CD8^+$ T cells were purified using RNeasy kit (QIAGEN). Reverse transcription was performed with QuantiTect Reverse Transcription kit (QIAGEN). Quantitative real-time PCR was performed on a Step-One Plus (Applied Biosystems) using TaqMan Low Density array (Applied Biosystems). RNA18S was used to normalize gene expression.

Statistical analyses

Results are expressed as means ± SEM or ranges, as appropriate. The Mann-Whitney test was used to compare two groups. The Kruskall-Wallis test was

used to compare three or more groups. Comparison between tumor growth curves have been performed using a two-way ANOVA test, and multiple comparisons have been corrected with the Bonferroni coefficient. Statistical significance was determined with Prism software (GraphPad Software). Significance was assumed at $P < 0.05$.

This work was supported by Roche, Pfizer, Association pour la Recherche contre le Cancer, Ligue contre le Cancer, and Association des Gastroentérologues Oncologues. TV was supported by Association Benoit Malassagne, Société Française de Chirurgie Digestive, and Assistance Publique - Hôpitaux de Paris (APHP - FERCM). M. Terme was supported by the Site de Recherche Intégré sur le Cancer-Programme Cancer Research for Personalized Medicine (CARPEM), the Association des Gastroentérologues Oncologues, and the Labex Immunooncology. S. Pernot and J. Taieb received a research grant from Roche. J. Taleb has an advisory role for Roche.

The authors declare no further conflicting financial interests.

Submitted: 24 March 2014
Accepted: 11 December 2014

REFERENCES

Adotevi, O., H. Pere, P. Ravel, N. Haicheur, C. Badoual, N. Merillon, J. Medioni, S. Peyrard, S. Roncelin, V. Verkarre, et al. 2010. A decrease of regulatory T cells correlates with overall survival after sunitinib-based antiangiogenic therapy in metastatic renal cancer patients. *J. Immunother.* 33:991–998. http://dx.doi.org/10.1097/CJI.0b013e3181f4c208

Appay, V., C. Jandus, V. Voelter, S. Reynard, S.E. Coupland, D. Rimoldi, D. Lienard, P. Guillaume, A.M. Krieg, J.-C. Cerottini, et al. 2006. New generation vaccine induces effective melanoma-specific CD8+ T cells in the circulation but not in the tumor site. *J. Immunol.* 177:1670–1678. http://dx.doi.org/10.4049/jimmunol.177.3.1670

Baitsch, L., P. Baumgaertner, E. Devêvre, S.K. Raghav, A. Legat, L. Barba, S. Wieckowski, H. Bouzourene, B. Deplancke, P. Romero, et al. 2011. Exhaustion of tumor-specific $CD8^+$ T cells in metastases from melanoma patients. *J. Clin. Invest.* 121:2350–2360. http://dx.doi.org/10.1172/JCI46102

Blackburn, S.D., H. Shin, W.N. Haining, T. Zou, C.J. Workman, A. Polley, M.R. Betts, G.J. Freeman, D.A.A. Vignali, and E.J. Wherry. 2009. Coregulation of CD8+ T cell exhaustion by multiple inhibitory receptors during chronic viral infection. *Nat. Immunol.* 10:29–37. http://dx.doi.org/10.1038/ni.1679

Cao, M., Y. Xu, J.I. Youn, R. Cabrera, X. Zhang, D. Gabrilovich, D.R. Nelson, and C. Liu. 2011. Kinase inhibitor Sorafenib modulates immunosuppressive cell populations in a murine liver cancer model. *Lab. Invest.* 91:598–608. http://dx.doi.org/10.1038/labinvest.2010.205

Dubreuil, P., S. Letard, M. Ciufolini, L. Gros, M. Humbert, N. Castéran, L. Borge, B. Hajem, A. Lermet, W. Sippl, et al. 2009. Masitinib (AB1010), a potent and selective tyrosine kinase inhibitor targeting KIT. *PLoS ONE.* 4:e7258. http://dx.doi.org/10.1371/journal.pone.0007258

Duraiswamy, J., K.M. Kaluza, G.J. Freeman, and G. Coukos. 2013. Dual blockade of PD-1 and CTLA-4 combined with tumor vaccine effectively restores T-cell rejection function in tumors. *Cancer Res.* 73:3591–3603. http://dx.doi.org/10.1158/0008-5472.CAN-12-4100

Finke, J.H., B. Rini, J. Ireland, P. Rayman, A. Richmond, A. Golshayan, L. Wood, P. Elson, J. Garcia, R. Dreicer, and R. Bukowski. 2008. Sunitinib reverses type-1 immune suppression and decreases T-regulatory cells in renal cell carcinoma patients. *Clin. Cancer Res.* 14:6674–6682. http://dx.doi.org/10.1158/1078-0432.CCR-07-5212

Gabrilovich, D.I., H.L. Chen, K.R. Girgis, H.T. Cunningham, G.M. Meny, S. Nadaf, D. Kavanaugh, and D.P. Carbone. 1996. Production of vascular endothelial growth factor by human tumors inhibits the functional maturation of dendritic cells. *Nat. Med.* 2:1096–1103. http://dx.doi.org/10.1038/nm1096-1096

Gavalas, N.G., M. Tsiatas, O. Tsitsilonis, E. Politi, K. Ioannou, A.C. Ziogas, A. Rodolakis, G. Vlahos, N. Thomakos, D. Haidopoulos, et al. 2012. VEGF directly suppresses activation of T cells from ascites secondary to ovarian cancer via VEGF receptor type 2. *Br. J. Cancer.* 107:1869–1875. http://dx.doi.org/10.1038/bjc.2012.468

Gibson, H.M., C.J. Hedgcock, B.M. Aufiero, A.J. Wilson, M.S. Hafner, G.C. Tsokos, and H.K. Wong. 2007. Induction of the CTLA-4 gene in human lymphocytes is dependent on NFAT binding the proximal promoter. *J. Immunol.* 179:3831–3840. http://dx.doi.org/10.4049/jimmunol.179.6.3831

Hamid, O., C. Robert, A. Daud, F.S. Hodi, W.-J. Hwu, R. Kefford, J.D. Wolchok, P. Hersey, R.W. Joseph, J.S. Weber, et al. 2013. Safety and tumor responses with lambrolizumab (anti-PD-1) in melanoma. *N. Engl. J. Med.* 369:134–144. http://dx.doi.org/10.1056/NEJMoa1305133

Huang, Y., X. Chen, M.M. Dikov, S.V. Novitskiy, C.A. Mosse, L. Yang, and D.P. Carbone. 2007. Distinct roles of VEGFR-1 and VEGFR-2 in the aberrant hematopoiesis associated with elevated levels of VEGF. *Blood.* 110:624–631. http://dx.doi.org/10.1182/blood-2007-01-065714

Ko, J.S., A.H. Zea, B.I. Rini, J.L. Ireland, P. Elson, P. Cohen, A. Golshayan, P.A. Rayman, L. Wood, J. Garcia, et al. 2009. Sunitinib mediates reversal of myeloid-derived suppressor cell accumulation in renal cell carcinoma patients. *Clin. Cancer Res.* 15:2148–2157. http://dx.doi.org/10.1158/1078-0432.CCR-08-1332

Le Roy, C., P.-A. Deglesne, N. Chevallier, T. Beitar, V. Eclache, M. Quettier, M. Boubaya, R. Letestu, V. Lévy, F. Ajchenbaum-Cymbalista, and N. Varin-Blank. 2012. The degree of BCR and NFAT activation predicts clinical outcomes in chronic lymphocytic leukemia. *Blood.* 120:356–365. http://dx.doi.org/10.1182/blood-2011-12-397158

Liu, Z.-J., T. Shirakawa, Y. Li, A. Soma, M. Oka, G.P. Dotto, R.M. Fairman, O.C. Velazquez, and M. Herlyn. 2003. Regulation of Notch1 and Dll4 by vascular endothelial growth factor in arterial endothelial cells: implications for modulating arteriogenesis and angiogenesis. *Mol. Cell. Biol.* 23:14–25. http://dx.doi.org/10.1128/MCB.23.1.14-25.2003

Oestreich, K.J., H. Yoon, R. Ahmed, and J.M. Boss. 2008. NFATc1 regulates PD-1 expression upon T cell activation. *J. Immunol.* 181:4832–4839. http://dx.doi.org/10.4049/jimmunol.181.7.4832

Ozao-Choy, J., G. Ma, J. Kao, G.X. Wang, M. Meseck, M. Sung, M. Schwartz, C.M. Divino, P.-Y. Pan, and S.-H. Chen. 2009. The novel role of tyrosine kinase inhibitor in the reversal of immune suppression and modulation of tumor microenvironment for immune-based cancer therapies. *Cancer Res.* 69:2514–2522. http://dx.doi.org/10.1158/0008-5472.CAN-08-4709

Sakuishi, K., L. Apetoh, J.M. Sullivan, B.R. Blazar, V.K. Kuchroo, and A.C. Anderson. 2010. Targeting Tim-3 and PD-1 pathways to reverse T cell exhaustion and restore anti-tumor immunity. *J. Exp. Med.* 207:2187–2194. http://dx.doi.org/10.1084/jem.20100643

Schreiber, R.D., L.J. Old, and M.J. Smyth. 2011. Cancer immunoediting: integrating immunity's roles in cancer suppression and promotion. *Science.* 331:1565–1570. http://dx.doi.org/10.1126/science.1203486

Schweighofer, B., J. Testori, C. Sturtzel, S. Sattler, H. Mayer, O. Wagner, M. Bilban, and E. Hofer. 2009. The VEGF-induced transcriptional response comprises gene clusters at the crossroad of angiogenesis and inflammation. *Thromb. Haemost.* 102:544–554.

Stockmann, C., A. Doedens, A. Weidemann, N. Zhang, N. Takeda, J.I. Greenberg, D.A. Cheresh, and R.S. Johnson. 2008. Deletion of vascular endothelial growth factor in myeloid cells accelerates tumorigenesis. *Nature.* 456:814–818. http://dx.doi.org/10.1038/nature07445

Terme, M., S. Pernot, E. Marcheteau, F. Sandoval, N. Benhamouda, O. Colussi, O. Dubreuil, A.F. Carpentier, E. Tartour, and J. Taieb. 2013. VEGFA-VEGFR pathway blockade inhibits tumor-induced regulatory T-cell proliferation in colorectal cancer. *Cancer Res.* 73:539–549. http://dx.doi.org/10.1158/0008-5472.CAN-12-2325

Topalian, S.L., F.S. Hodi, J.R. Brahmer, S.N. Gettinger, D.C. Smith, D.F. McDermott, J.D. Powderly, R.D. Carvajal, J.A. Sosman, M.B. Atkins, et al. 2012. Safety, activity, and immune correlates of anti-PD-1 antibody in cancer. *N. Engl. J. Med.* 366:2443–2454. http://dx.doi.org/10.1056/NEJMoa1200690

Wherry, E.J. 2011. T cell exhaustion. *Nat. Immunol.* 12:492–499. http://dx.doi.org/10.1038/ni.2035

Published January 19, 2015

Wherry, E.J., S.-J. Ha, S.M. Kaech, W.N. Haining, S. Sarkar, V. Kalia, S. Subramaniam, J.N. Blattman, D.L. Barber, and R. Ahmed. 2007. Molecular signature of CD8+ T cell exhaustion during chronic viral infection. *Immunity*. 27:670–684. http://dx.doi.org/10.1016/j.immuni.2007.09.006

Whiteside, T.L., and G. Parmiani. 1994. Tumor-infiltrating lymphocytes: their phenotype, functions and clinical use. *Cancer Immunol. Immunother.* 39:15–21. http://dx.doi.org/10.1007/BF01517175

Woo, S.-R., M.E. Turnis, M.V. Goldberg, J. Bankoti, M. Selby, C.J. Nirschl, M.L. Bettini, D.M. Gravano, P. Vogel, C.L. Liu, et al. 2012. Immune inhibitory molecules LAG-3 and PD-1 synergistically regulate T-cell function to promote tumoral immune escape. *Cancer Res.* 72:917–927. http://dx.doi.org/10.1158/0008-5472.CAN-11-1620

Yamazaki, T., H. Akiba, A. Koyanagi, M. Azuma, H. Yagita, and K. Okumura. 2005. Blockade of B7-H1 on macrophages suppresses CD4+ T cell proliferation by augmenting IFN-gamma-induced nitric oxide production. *J. Immunol.* 175:1586–1592. http://dx.doi.org/10.4049/jimmunol.175.3.1586

Ziogas, A.C., N.G. Gavalas, M. Tsiatas, O. Tsitsilonis, E. Politi, E. Terpos, A. Rodolakis, G. Vlahos, N. Thomakos, D. Haidopoulos, et al. 2012. VEGF directly suppresses activation of T cells from ovarian cancer patients and healthy individuals via VEGF receptor Type 2. *Int. J. Cancer.* 130:857–864. http://dx.doi.org/10.1002/ijc.26094